

RESEARCH ARTICLE

# A crowd route choice evacuation model in large indoor building spaces



Y. Wu<sup>a,c,\*</sup>, J. Kang<sup>a,b,c</sup>, C. Wang<sup>b,c</sup>

<sup>a</sup>School of Architecture, Harbin Institute of Technology, Harbin 150001, PR China

<sup>b</sup>School of Architecture, University of Sheffield, Sheffield S10 2TN, UK

<sup>c</sup>School of Architecture, Tianjin University, Tianjin 300072, PR China

Received 16 February 2017; received in revised form 26 February 2018; accepted 1 March 2018

## KEYWORDS

Crowd;  
Evacuation;  
Cellular automaton  
model;  
Sound;  
Voice warning system

## Abstract

Route choice is a fundamental requirement in the evacuation process. The aim of this paper is to identify a method to simulate crowds in large indoor spaces with consideration of the acoustic system. This paper first extends an existing cellular automaton model and proposes a cellular automaton crowd route choice model (CACR model) to simulate evacuees in large indoor spaces. It then defines a measure for evaluating the utility of evacuation time using the CACR model under different circumstances, such as a fire situation or different voice warning systems, which other commercial models cannot simulate. The analysis of the characteristics of a sound field in large indoor spaces is based on field measurements. An observation experiment in a gymnasium is employed to test the proposed model in a stadium evacuation scenario. The results demonstrate that the CACR model can accurately simulate the evacuation process in large indoor spaces under various circumstances.

© 2018 The Authors. This is an open access article under the CC BY-NC-ND license (<http://creativecommons.org/licenses/by-nc-nd/4.0/>).

## 1. Introduction

The evacuation process is very complicated considering the variety of individual features. Previous research work has been

developed on two aspects, evacuation time (Gwynne et al., 1999; Ashe and Shields, 1999) and human behaviour (Sekizawa et al., 1999; Sime, 2001). The evacuation time consists of pre-movement and movement time. It is a common practice to set the pre-movement time in the calculations according to past experience as an effort to avoid too much deviation (Gwynne et al., 1999). Attention has also been paid to research on formulas for and models of movement time (Ashe and Shields, 1999). On the other hand, investigation of human psychology and behaviour plays an important role in the research on

\*Corresponding author at: School of Architecture, Harbin Institute of Technology, No. 66 West Dazhi Street, Harbin 150001, PR China.

E-mail address: [wuyuehit@hit.edu.cn](mailto:wuyuehit@hit.edu.cn) (Y. Wu).

Peer review under responsibility of Southeast University.

evacuation efficiency. Three interactions will have important influence on decisions individuals make during evacuation: interactions between people, between people and architecture, and between people and the environment (Yang et al., 2005). Human cognitive behaviour will influence the evacuation process in emergency situations (Pires, 2005).

Further research has found that different building styles may cause polytropic evacuation processes. This finding has made research on evacuation times and human behaviour more diversified and closer to actual experience (Tong and Canter, 1985; Fang et al., 2011; Zheng et al., 2010). For instance, large building spaces such as airports, railway stations, libraries, gymnasiums, and exhibition halls (Shi et al., 2009a) have large capacities and long and complex pedestrian routes. Due to the spatial conditions of these large open buildings, smoke may influence the evacuation direction and cause delays in the evacuation time, especially in the case of a fire. For this reason, the research field has been extended, and multiple-factor models have been developed based on basic research on evacuation time and human behaviour mentioned above (Kobes et al., 2010; Pu and Zlatanova, 2005; Pereira et al., 2013). Zheng reviewed the basic models for evacuation simulations (Fang et al., 2011), including cellular automaton (CA) models, lattice gas models, social force models, fluid-dynamic models, agent-based models, game theory models, and models based on animal experiments, as the basis for evacuation simulations. The connection between the environment and evacuation has been considered in these models.

Jeon and Hong (2009) and Kobes (2010) studied human movement when visibility is decreased in evacuation experiments. Further research has found that sound plays an important role in the evacuation process. Bryan (2002) found that acoustic signals indicate danger, especially in a fire situation. Bruck discussed the influence of 13 factors on responsiveness during sleep and proposed consideration of the situation, sound pressure level and frequency in the installation of fire alarms (Bruck, 2001). Ramachandran (1991) proposed that a high-frequency alarm tone notably reduces pre-evacuation time. Previous research has considered environmental information, uncertainties in evacuation time (Jeon and Hong, 2009; Kobes, 2010), and the choice of route and human behaviour under voice guidance (Bryan, 2002; Bruck, 2001; Ramachandran, 1991). However, further studies are necessary to address uncertainties by introducing additional influential factors into the evacuation model.

The aim of this paper is to develop a method to simulate a crowd's evacuation process in large indoor spaces and to propose the integration of a voice warning system (VWS) into emergency systems. The paper first develops a numerical simulation model, the cellular automaton crowd route choice model (CACR model) based on the CA model, to describe a crowd's evacuation process. It then explores each variable used in the model, including some indefinite variables that are determined by evacuation experiments and sound-field tests. Experimental data from an observation experiment are used to validate the CACR model.

## 2. Numerical simulation model

In this section, the CA model is chosen as the original model in which each cell evolves according to the way it interacts

with its neighbours. Some rules have been reset, and the model has been extended. The CACR model has been developed as follows. First, according to the operating rules of the CA model, the influence of static and dynamic information attraction on the crowd's route choice is added. Second, the numerical simulation model is developed. Finally, the model and each variable are explained. Some key variables are discussed along with the experiments in Section 3.

### 2.1. Basic model

Many models have been developed to provide designers with ways of forecasting evacuation times for buildings (Fang et al., 2011). Based on dynamics theory, the evacuation process is described as a process in which the actions of agent objects are influenced by various factors as time progresses. A numerical model and certain rules simulate the different behaviours and features of an individual in the evacuation process. The building plan can be divided into uniform grids. Each grid is occupied by a wall, another obstacle, a human, or is free (Shi et al., 2009b). The CACR model, which is an agent-based evacuation simulation program, was developed based on one of the microscopic models, the CA model, which includes the spatial environment. The CACR model utilizes the CA model to synchronously update static and dynamic information at all times (e.g., visibility, voice commands).

Models for simulation can be classified into two categories: macroscopic and microscopic. Macroscopic models focus on people and the building as a whole system, whereas microscopic models study the behaviour and decisions of individual people and their interaction with other people in crowds. Macroscopic models include regression models (Milazzo et al., 1998), route choice models (Lovas, 1994), queuing models (Hoogendoorn and Bovy, 2003), and gas-kinetics models (Henderson, 1971). Microscopic models include social forces (particle systems) (Helbing et al., 2000), rule-based models (Wolfgram, 1983), and cellular automata models (Nuria and Ali, 2008).

Because microscopic models can consider the behaviour and decisions of individual people within the models, they are commonly used to simulate crowd evacuations. The crowd's route choice model in this paper requires one basis model from these microscopic models. The main difference between the microscopic models is whether they treat the space as continuous (social forces and rule-based) or discrete (CA). Social forces and rule-based models are used for multiple-spatial buildings, whereas a CA model is used for simple spatial buildings. Thus, to simulate evacuation in large indoor spaces, the CA model has been chosen.

### 2.2. CACR model

Based on the fundamental rules of the CA model, it is assumed that each person has a  $0.4 \times 0.4 \text{ m}^2$  space, which is the typical spatial distribution in public crowded spaces (Burstedde et al., 2001). The location of a person is expressed in terms of rows and columns (i,j). Each cell contains one person who can move only one cell adjacently in one time step. A building plan can be represented as an

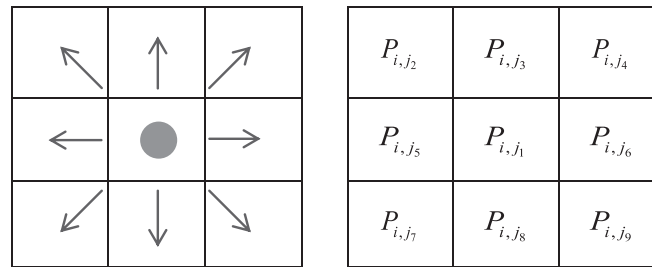


Figure 1 Movable probability distribution.

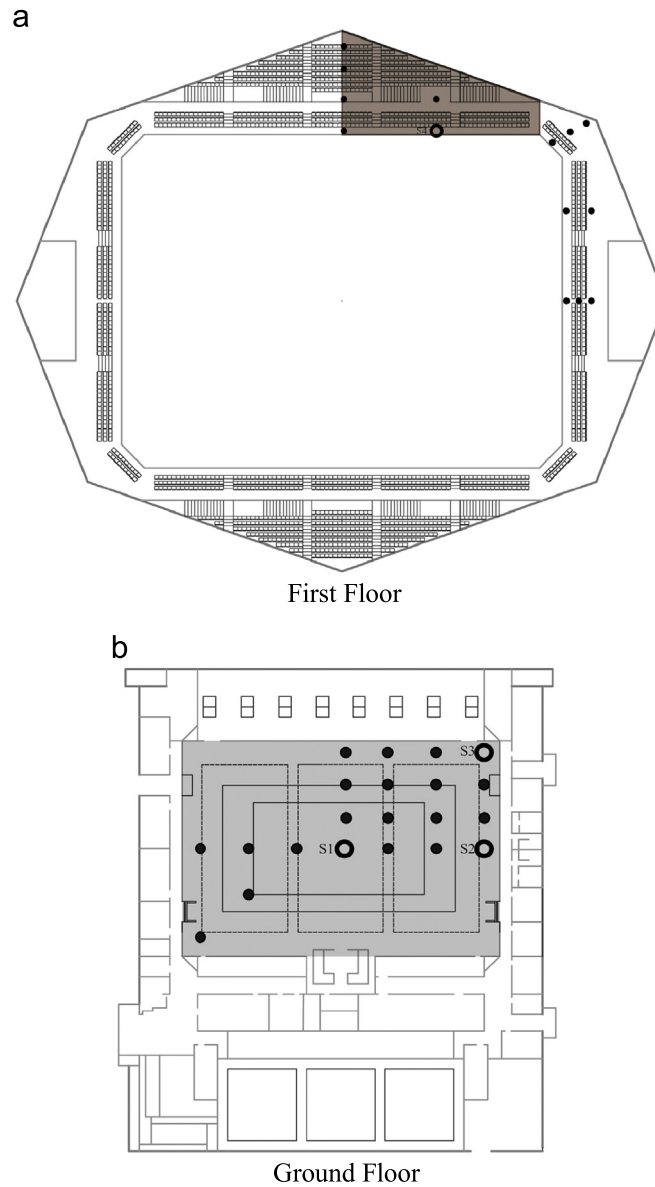
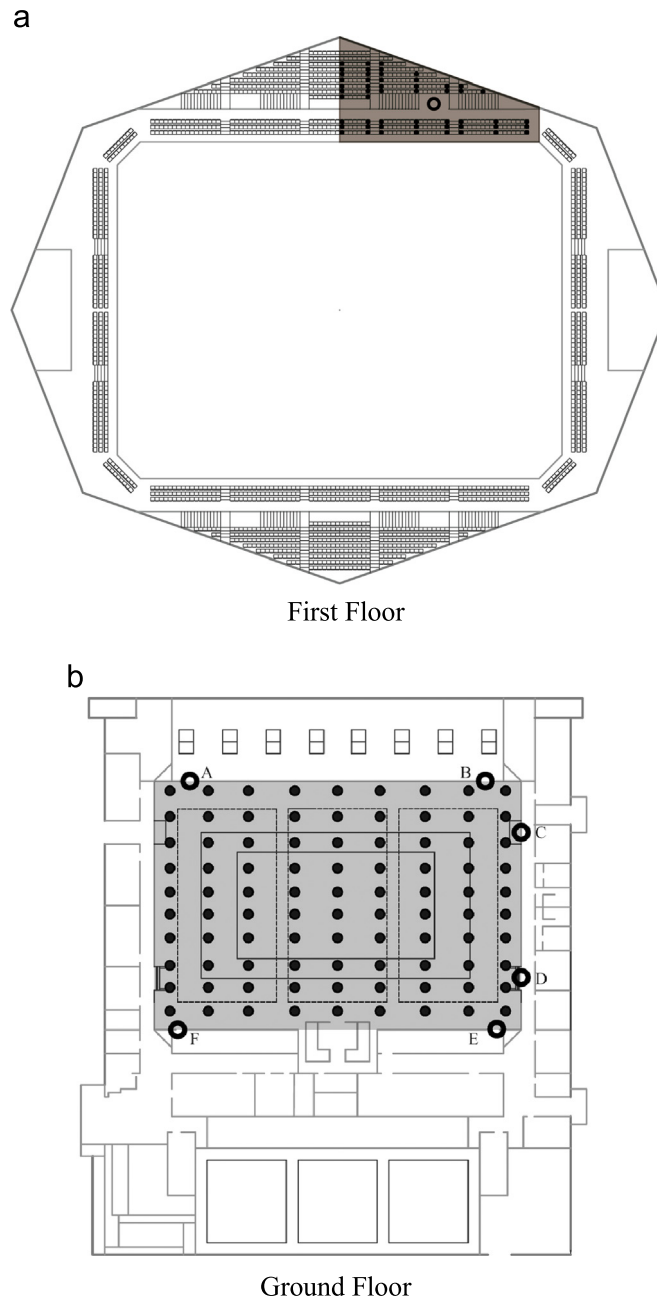


Figure 2 Plans of the gym.

$n \times n$  plan matrix. Each position  $(i,j)$  of this matrix has a value of 1 when filled with a person and 0 when it is empty. Moving from position  $(i,j)$  to position  $(i,j + 1)$  indicates that the position of a person has changed one step further. In the CACR model, the Moore neighbourhood has been selected as the neighbourhood of each person to simplify the calculation, and each cell contains multiple persons, referred to as

a “group”. Figure 1 shows the movable probability distribution. Each time step represents different real times of evacuation based on different movement velocities of the occupant (Zhao et al., 2008).

Define  $n_j$  as the current quantity to accommodate in grid  $j$  and  $n_{max}$  as the maximum quantity to accommodate in grid  $j$ . Define  $M$  as the grid number of plane segmentation in the



**Figure 3** Evacuees (dots) and exit positions (circles) in the evacuation experiment.

building. When  $n_j$  exceeds this value, evacuees in the same grid would impede each other. The variables  $n_j$  and  $n_{max}$  are input values needed before simulation.  $P_{i,j}$  shows the probability of evacuees in group  $i$  moving to grid  $j$  at the next time step. Association probabilities can be expressed with the following formula:

$$P_{i,j} = \frac{\exp\{k_S \cdot S_{i,j} + k_D \cdot D_{i,j}\} \cdot (n_{max} - n_j)}{\sum_{j \in M} [\exp\{k_S \cdot S_{i,j} + k_D \cdot D_{i,j}\} \cdot (n_{max} - n_j)]}, \quad (1)$$

where  $k_D$  is the weighting coefficient of the dynamic information attraction.  $S_{i,j}$  and  $D_{i,j}$  are the static information attraction and dynamic information attraction from grid  $j$  to evacuees  $i$ .

At each time step, each group follows the three rules below to determine the next step.

- (1) Each group can feel the state only within a certain visual field. Each agent uses the route selection formula expressed above to choose the next target grid.
- (2) The model assumes that one grid can contain multiple agents at one time step, referred to as a “group”, and one grid has its own maximum accommodation quantity. If the number of agents exceeds the maximum accommodation as they move to the same grid (which means a conflict), some agents will either stay at the original grid or move to the side to try to bypass.
- (3) All agents should be judged regardless of whether they have arrived at the exit. If not, the new position of every

**Table 1** The static and dynamic information and evacuation comparisons of fifty evacuees under evacuation simulation with a single source on the first floor of the gymnasium.

Evacuee	Route length (m)	Evacuation time (s)	Scenario 1	Scenario 2	Scenario 3	Scenario 4
E1	14		19.2	16.3	28.3	24.0
E2	10		13.8	12.0	21.0	18.0
E3	10		13.6	11.8	20.7	17.8
E4	13.5		18.3	15.5	26.8	22.7
E5	9.5		13.8	11.9	20.9	17.9
E6	9.5		14.0	12.2	21.3	18.3
E7	13		17.3	14.6	25.4	21.4
E8	9		12.5	10.8	19.0	16.3
E9	9		12.2	10.6	18.5	15.9
E10	13		17.2	14.6	25.2	21.3
E11	12.5		14.8	12.4	21.5	18.2
E12	8.5		12.0	10.4	18.1	15.5
E13	8.5		11.8	10.2	17.8	15.2
E14	12.5		15.3	12.9	22.3	18.8
E15	12		15.0	12.6	21.8	18.4
E16	8		10.5	9.1	15.8	13.5
E17	8		10.3	8.8	15.4	13.2
E18	16		17.7	14.7	25.3	21.1
E19	12		12.6	10.6	18.3	15.4
E20	13		12.0	10.1	17.4	14.6
E21	11.5		14.3	12.0	20.6	17.3
E22	7.5		9.4	8.1	14.1	12.0
E23	7.5		9.3	8.0	13.9	11.8
E24	15.5		16.3	13.5	23.1	19.3
E25	11.5		10.8	9.0	15.6	13.1
E26	12.5		10.5	8.8	15.1	12.7
E27	16.5		14.8	12.2	20.9	17.4
E28	11		12.7	10.6	18.3	15.4
E29	7		8.5	7.3	12.7	10.8
E30	11		7.7	6.2	10.4	8.5
E31	7		3.8	3.0	5.1	4.1
E32	6		3.5	2.8	4.7	3.9
E33	7		5.6	4.5	7.6	6.2
E34	3		1.8	1.4	2.4	1.9
E35	3		1.7	1.4	2.3	1.9
E36	7		5.5	4.4	7.4	6.1
E37	11.5		8.6	7.0	11.7	9.6
E38	7.5		4.3	3.6	5.8	4.8
E39	6.5		4.5	3.7	6.1	5.1
E40	7.5		6.3	5.1	8.5	7.0
E41	3.5		2.3	1.9	3.1	2.6
E42	3.5		2.7	2.2	3.7	3.1
E43	7.5		6.3	5.1	8.5	7.0
E44	12		9.5	7.8	13.0	10.7
E45	8		5.1	4.3	7.0	5.8
E46	7		5.4	4.5	7.4	6.2
E47	8		8.5	6.8	11.7	9.7
E48	4		3.2	2.6	4.5	3.8
E49	4		3.4	2.7	4.8	4.0
E50	8		9.5	7.5	13.1	10.8

According to the rule, in scenario 1,  $k_D = 0$ , in scenario 2,  $k_D = 0.84$ , in scenario 3,  $k_D = 1.43$ , and in scenario 4,  $k_D = 1.2$ .

**Table 2** The obstruction length and evacuation comparisons of fifty evacuees under evacuation simulation with multiple sources on the ground floor of the gymnasium.

Evacuee	Route length (m)	Total	Down-stairs	Up-stairs	Flat	Evacuation speed (m/s)
E1		14	7	0	7	0.73
E2		10	7	0	3	0.73
E3		10	7	0	3	0.74
E4		13.5	6.5	0	7	0.74
E5		9.5	6.5	0	3	0.69
E6		9.5	6.5	0	3	0.68
E7		13	6	0	7	0.75
E8		9	6	0	3	0.72
E9		9	6	0	3	0.74
E10		13	6	0	7	0.76
E11		12.5	5.5	0	7	0.85
E12		8.5	5.5	0	3	0.71
E13		8.5	5.5	0	3	0.72
E14		12.5	5.5	0	7	0.82
E15		12	5	0	7	0.80
E16		8	5	0	3	0.76
E17		8	5	0	3	0.78
E18		16	5	0	11	0.90
E19		12	5	0	7	0.95
E20		13	5	0	8	1.08
E21		11.5	4.5	0	7	0.81
E22		7.5	4.5	0	3	0.80
E23		7.5	4.5	0	3	0.81
E24		15.5	4.5	0	11	0.95
E25		11.5	4.5	0	7	1.07
E26		12.5	4.5	0	8	1.19
E27		16.5	4.5	0	12	1.12
E28		11	4	0	7	0.87
E29		7	4	0	3	0.82
E30		11	0	0	11	1.43
E31		7	0	0	7	1.87
E32		6	0	0	6	1.71
E33		7	0	0	7	1.25
E34		3	0	0	3	1.71
E35		3	0	0	3	1.76
E36		7	0	0	7	1.27
E37		11.5	0	0.5	11	1.34
E38		7.5	0	0.5	7	1.76
E39		6.5	0	0.5	6	1.44
E40		7.5	0	0.5	7	1.20
E41		3.5	0	0.5	3	1.56
E42		3.5	0	0.5	3	1.30
E43		7.5	0	0.5	7	1.20
E44		12	0	1	11	1.26
E45		8	0	1	7	1.57
E46		7	0	1	6	1.30
E47		8	0	1	7	0.94
E48		4	0	1	3	1.25
E49		4	0	1	3	1.18
E50		8	0	1	7	0.84

agent will be decided again at the next time step. Finally, if an agent has moved to a safe place, this agent will be no longer participating in the evacuation process.

In the numerical expression of the CACR model, there are three unknown variables;  $k_D$  differs in different simulation scenarios. It needs to be determined by experimental results, which will be discussed in Section 4.  $S_{i,j}$  and  $D_{i,j}$  are influenced by many aspects, which are discussed in Sections 2.3 and 2.4.

### 2.3. Static information attraction $S_{i,j}$

As mentioned in Eq. (1),  $S_{i,j}$  is the static information attraction from grid  $j$  to agent  $i$ , which indicates the safety factor of the agent inside the space assuming the space position information remains unchanged, including the location of obstacles (such as chairs or tables) and physical boundaries (such as doors or walls).

Define  $S_{i,j} = a_{i,e_k} \cdot r_{i,j}$ , (2)

where  $a_{i,e_k}$  is the hindrance factor, namely, the hindrance degree of the walls and stairs on occupant  $i$  to exit  $e_k$ .

$$a_{i,e_k} = \alpha \frac{r_f}{r_{i,j}} + \beta \frac{r_s}{r_{i,j}}, \quad (3)$$

where  $r_f$  is the horizontal distance from grid  $j$  to exit  $e_k$ , and  $r_s$  is the slope length of the stairs from grid  $j$  to exit  $e_k$ .  $\alpha$  and  $\beta$  are the coefficients of the obstruction factor; the values of  $\alpha$  and  $\beta$  are discussed in Section 4.2.  $r_{i,j}$  is the distance from grid  $j$  to exit  $e_k$ .

$$r_{i,j} = \max_{(i,j)} \left\{ \min_{e_k} \left[ \left| x_j - x_{e_k} \right| + \left| y_j - y_{e_k} \right| \right] \right. \\ \left. - \min_{e_k} \left[ \left| x_j - x_{e_k} \right| + \left| y_j - y_{e_k} \right| \right], \right. \quad (4)$$

where  $(x_j, y_j)$  is the current position coordinate and  $(x_{e_k}, y_{e_k})$  is the exit position coordinate.

The static information attraction includes many factors. They involve all physical factors that relate to safety evaluation, and they remain stable through the evacuation process. Rules targeted at a single evacuee can be chosen in the evacuation simulation.

### 2.4. Dynamic information attraction $D_{i,j}$

$D_{i,j}$  is the dynamic information attraction from grid  $j$  to agent  $i$ . Some physical qualities are altered in the evacuation process. For instance, the voice warning system and luminance affect the estimate of dynamic information in one grid from one agent. The formula is shown as below:

$$\text{Define } D_{i,j} = b_{i,j} \cdot f_{i,w_k}(t), \quad (5)$$

where  $b_{i,j}$  is a subjective characteristic, such as personal experience and fire science education, which influences the reaction of people under fire conditions. The value can reference a relevant survey statistics report or the probability distribution.

$f_{i,w_k}(t)$  is the objective characteristic at the current moment, such as acoustic alarm information or visibility in the environment.

$$f_{i,w_k}(t) = g_{i,j}(t) \cdot [\theta_{i,j} \cdot l_{i,w_k}(t)], \quad (6)$$

where  $g_{i,j}(t)$  is the coefficient of visibility conditions,  $0 < g_{i,j}(t) < 1$ , using a Gaussian distribution where  $x$  is random variable,  $x \sim N(\mu, \sigma^2)$ .

$$g_{i,j}(t) = \frac{1}{\sqrt{2\pi}\sigma} e^{-\frac{(x-\mu)^2}{2\sigma^2}} (\sigma > 0), \quad (7)$$

where  $l_{i,w_k}(t)$  is the weight of the VWS. The weight of the VWS to a person depends on the value of  $L_w$  (sound power level) in the current position and the reverberation time  $T_{60}$  in the space. Actual measurements in Section 3.2 are compared with calculation results in Section 4.3 to ensure the correct determination of the value of  $l_{i,w_k}(t)$ .

### 2.5. Additional rules

This model focuses on the influence of environmental information on the evacuation process. Although not all factors are considered, the model described in Section 2.2 is an open-type model. Additional factors, such as those discussed below, can be taken into account when needed.

#### 2.5.1. Status of evacuees

Responsiveness influences the reception and handling ability. The value of  $a_{i,e_k}$  should not be ignored, especially in simulations of particular types of spaces, such as hospitals and intensive care spaces. According to previous research (Mac et al., 1999), a Weibull distribution can be chosen.

#### 2.5.2. Interaction between evacuees

In the evacuation process, interactions such as attraction, repulsive force and friction exist among evacuees. Because the model considers environmental information separately, it does not include interactions. However, if friction needs to be considered, the "friction factor"  $\exp\{k_f \cdot F_{i,j}\}$  can be added into formula (1). The value  $k_f$  is the friction coefficient, and  $F_{i,j}$  is the normal force from the agent in grid  $j$  to the agent in grid  $i$ .

## 3. Experimental method

An experiment was conducted to determine the unknown variables in the CACR model in Section 2: the weighting coefficient  $k_D$  in Eq. (1),  $\alpha$  and  $\beta$  in Eq. (2), and the weight of VWS  $l_{i,w_k}(t)$  in Eq. (6). Therefore, the experiment is divided into two parts. One part is the evacuation experiment, shown in Section 3.2, which considers  $k_D$ ,  $\alpha$  and  $\beta$ . The other part is the acoustic experiment, shown in Section 3.3, which considers  $l_{i,w_k}(t)$ .

### 3.1. Case study space

The building containing the large space for the case study is the gymnasium of the Harbin Institute of Technology. Officially opened in 1995, the building has two floors. The

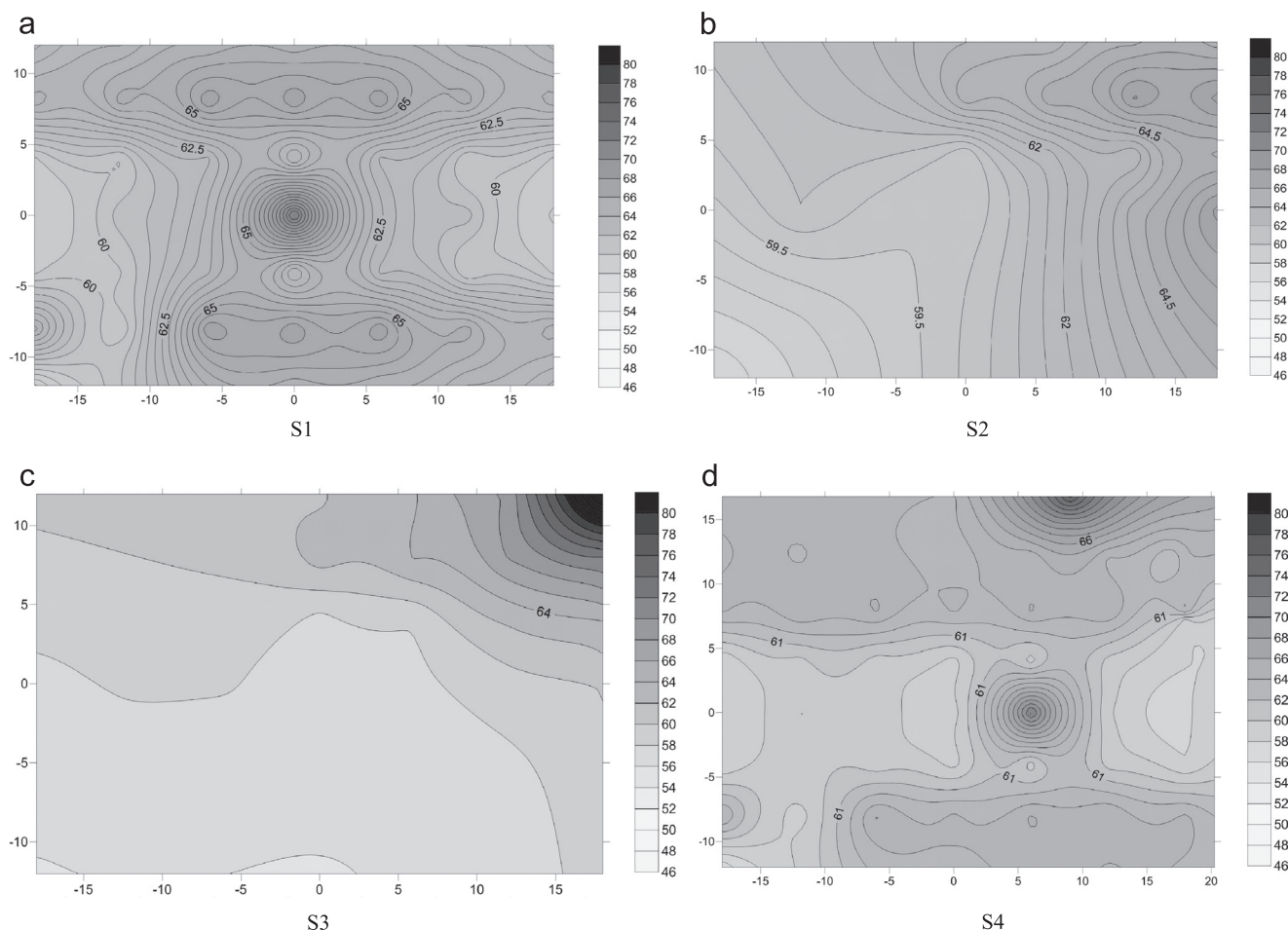


**Figure 4** The SPL distribution of S1-S4 at typical frequencies 2 kHz.

first floor area is 6300 m<sup>2</sup>, and the ground area is 10,000 m<sup>2</sup>. The facility is composed of a 3000-seat auditorium and a competition area with three basketball courts. [Figure 2](#) shows the building plans. There are corridors surrounding the courts leading to offices and an equipment room.

### 3.2. Evacuation experiments

Fifty evacuees were tested on the first floor by changing the condition of visibility and changing whether the VWS was on or off. Since it is difficult to conduct evacuation experiments in a stadium that can accommodate thousands of people, a simplification method was adopted. In [Section 2.5](#), there are additional rules so that interactions between people can be ignored in the basic model. Evacuees were tested in each row of the audience, one near the evacuation walk and another in the middle of the audience. Seventy evacuees were tested on the ground floor by changing the visibility condition and the number of VWSs to simplify the calculation and prevent people's behaviour from being affected by others. The stadium was divided into multiple cells. Each cell contained one person, and each person had a 4 × 4 m<sup>2</sup> space.

#### 3.2.1. Evacuation with a single sound source

This study discusses the characteristics and changes of an evacuee's behaviour under the visual conditions found in a

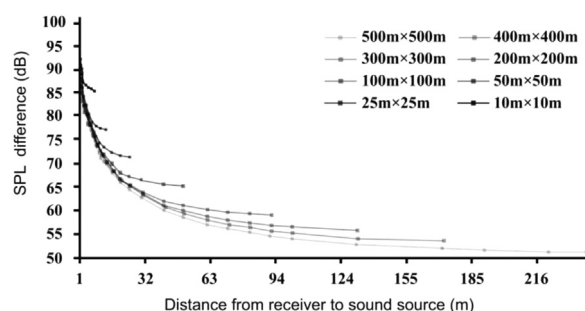


**Figure 5** SPL changing with the variation of distance using numeric calculation and Odeon simulation.

fire situation where the space is filled with smoke. Voice is the single area discussed as smoke only impacted visibility. Previous research that has considered other impacts on evacuation speed is ignored ([Jin, 2008](#); [Frantzych and Nilsson, 2003](#); [Ronchi et al., 2013](#)). The individual evacuation activities of the fifty evacuees were recorded and analysed. [Figure 3](#) shows the evacuees' positions. Due to the symmetrical space, the quarter of the gym on the first floor was considered an experiment field, as shown in [Figure 2\(b\)](#) (shadowed areas). Differences regarding evacuation times, movement speed, evacuation routes and travel distance were studied under different visibility conditions. In addition, the evacuees' subjective responses and

acknowledgement of the acoustic guidance signs are addressed in this paper.

It is difficult to address complicated variable lighting, so the evacuees were blindfolded to simulate a smoke-filled space. The evacuees began in the seating area on the first floor and evacuated to the exit of this floor (shown in Figure 3-b, marked as a circle) one at a time. The time and the route were recorded.

Evacuation under a high visibility condition in the fire is classified in scenarios 1 and 2 based on the on-off state of the VWS. Scenario 1 is when the system is off, and scenario 2 is when it is on. A whistling voice was used to simulate the emergency acoustic voice. Evacuation under a low visibility condition in the fire is classified in scenarios 3 and 4 based on the on-off state of the VWS. Scenario 3 is when the system is off, and scenario 4 is when the voice warning system is on.

Two other evacuation observation experiments were conducted with different numbers of evacuees and different dynamic information. Test A had 100 people evacuating at the same time, and test B had 200 people evacuating. The evacuation time was recorded.

### 3.2.2. Evacuation with multiple sound sources

In general, there are multiple evacuation alarm sources in a building with a large open space. To determine the actual situation, experiments using multiple alarm sources were conducted. In these experiments, the characteristics and changes of each evacuee's behaviour under VWS influence were examined. The individual evacuation activities of the seventy evacuees were recorded and analysed. Figure 3-b shows the evacuees' positions. Again, a quarter of the ground floor was taken as the experiment field, shown in Figure 2(a) (shaded areas). The differences regarding the choice of exit were studied with different numbers of loudspeakers. Three evacuation observation experiments were conducted with different numbers of evacuees and different dynamic information. Test A had 70 people evacuate at the same time, test B had 150 people, and Test C had 300 people. The evacuation time and the choice of exits were recorded.

### 3.3. Sound field measurements

This section tests the building's acoustic environment and obtains the sound pressure level values at a number of locations throughout the building to verify that the actual situation is consistent with the theoretical calculation values.

The measurement was designed to examine the sound field in detail. As illustrated in Figure 2, four sound source positions (circles), marked as S1-S4, were considered; three were on the ground floor and one was on the first floor. On the ground floor, one source position was considered in the middle of the gym (S1), one along the short side of the court (S2) and the other near a corner that was also an exit (S3), shown in Figure 2-b. On the first floor, the source (S4) was positioned at a similar plan location as S3 near a staircase to the ground floor, shown in Figure 2-a. The sound source was an omni-directional source using a cluster of 12 loudspeakers in a dodecahedral configuration that radiates sound

evenly with spherical distribution. The acoustic power level was 109.99 dB, and it was set in the centre of the space 1.5 m above the ground. For a given source position, 36 receiver positions that were generally evenly distributed across the space with a spacing of 3-8 m were considered. However, some special locations were also taken into account, such as the points at the exits as well as some points near the staircase. The distribution of the receiver positions is shown in Figure 2. Equipment used to measure and record the sound at the receivers included both Type I sound level metres and digital sound recorders.

## 4. Determinant of unknown variables in the numerical model

Based on the experiments, the weighting coefficient  $k_D$  in Eq. (1), the coefficient of obstruction factors  $\alpha$  and  $\beta$  in Eq. (2) and the weight of VWS  $l_{i,w_k}(t)$  in Eq. (6) are discussed.

### 4.1. Weighting coefficient $k_D$

Static information represents the obstacles in the space. It does not change with respect to time. In this paper, static information represents stairs. Dynamic information represents different visibility conditions or the on-off state of the voice warning system, which may change with time.

In scenario 1, with the alarm off and high visibility,  $k_D = 0$ , which means the route selection is only influenced by static information. The coefficient  $k_D$  increases with an increase in dynamic information attraction. This means the route selection depends on the dynamic information incidence, as shown in Table 1.

However, in a gym evacuation, thousands of people are evacuating at the same time. Since the number of people involved can greatly alter the situation, the number of people being evacuated needs to be discussed. With an increase in the number of evacuees, interactions such as attraction, repulsive force, and friction exist among evacuees, and the evacuation time is extended. Because the model considers environmental information separately, it does not include interactions. However, if friction needs to be considered, the "friction factor"  $\exp\{k_f \cdot F_{ij}\}$  can be added into formula (1).

$$P_{ij} = \frac{\exp\{k_S \cdot S_{ij} + k_D \cdot D_{ij} + k_f \cdot F_{ij}\} \cdot (n_{max} - n_j)}{\sum_{j \in M} [\exp\{k_S \cdot S_{ij} + k_D \cdot D_{ij} + k_f \cdot F_{ij}\} \cdot (n_{max} - n_j)]} \quad (8)$$

Two evacuation observation experiments were tested with different numbers of evacuees and changing dynamic information. Test A had 100 people evacuating at the same time, and test B had 200 people. The evacuation time was recorded. We discuss and calculate the weighting coefficient  $k_D$  and obtain results consistent with the observational data of 50 evacuees. Formula (8) is workable.

### 4.2. Coefficient of obstruction factors $\alpha$ and $\beta$

The coefficient  $a_{i,e_k}$  is the hindrance factor, as mentioned in Section 2.3, and is the level of hindrance from walls and stairs upon agent  $i$  to exit  $e_k$ . Eq. (3) shows that the same evacuation speed means the same value for  $a_{i,e_k}$ , so the

value of  $\alpha$  and  $\beta$  can be calculated using the obstruction length recorded in the evacuation experiment.

Table 2 shows the route length of the evacuation process of each evacuee in the experiment in Section 3.2 based on the recorded evacuation time used to calculate the evacuation speed of each evacuee.

Because S2, S3 and S4, as well as S1 and S6, show the same speed under alarm-off and high visibility conditions, the data were chosen to calculate the best values of  $\alpha$  and  $\beta$ , giving  $\alpha = 1.12, \beta = 0.89$ . Two evacuation observation experiments were tested with different numbers of evacuees and changing static information. Test A had 100 people evacuating at the same time, and test B had 200 people. The evacuation time was recorded. We discuss and calculate the coefficient of obstruction factor  $\alpha$  and  $\beta$  and obtain results consistent with the observational data of 50 evacuees because the interactions between evacuees are considered in formula (8) by adding the friction factor.

### 4.3. VWS weight $l_{i,w_k}(t)$

The sound of the voice from the voice warning alarm actually heard by humans is mainly affected by two aspects: the sound pressure level from the sound source at the receivers' positions and the reverberation time in the space.

#### 4.3.1. Sound pressure level

Under normal conditions, the alarm source is a point source, and the total sound pressure level at a receiver point can be calculated by

$$l_{i,w_k}(t) = \ln \left[ L_w + 10 \lg \left( \frac{Q}{4\pi r^2} + \frac{4}{R} \right) \right], \quad (9)$$

where  $Q$  is the source directivity factor,  $r$  is the distance from the test point to the sound source, and  $R$  is a constant of the room  $R = \frac{s\bar{\alpha}}{1-\bar{\alpha}}$ , where  $s$  is the total superficial area and  $\bar{\alpha}$  is the average sound absorption coefficient.

To determine how  $L_w$  changes with  $r$  in large spaces, eight rectangular spaces are calculated below. The sound source is an omnidirectional source, and the sound power level is 109.99 dB and is set in the centre of the model 1.5 m above the ground. Side lengths are 10 m, 25 m, 50 m, 100 m, 200 m, 300 m, 400 m and 500 m. The sound absorption coefficient is 0.2, and the diffusion coefficient is 0.05. Receivers are set along a row of test points to simulate the height of the human ear. The length of the space increases from 10 m to 500 m. Figure 4 shows the sound pressure level at 1 kHz using numeric calculations and field measurements. It can be seen that for the calculated results, the sound field in a large space is similar to a semi-free sound field. When  $s$  becomes very large, asymptotically approaches zero. The sound pressure levels decay rapidly with an increase in the distance from the sound source. The variable  $L_w$  decreases exponentially with  $r$ , the distance from the receiver to the sound source. Figure 5 shows the sound pressure level (SPL) distribution on the ground floor (S1-S3) and the first floor (S4) of each source position based on the experiment results in Section 3.3 at typical frequencies of 2 kHz. The sound pressure level decreases with increasing distance to the source, again similar to the semi-free sound field. This suggests the semi-free characteristics of a typical large space. Overall, the results show that the actual measurement results and the calculated results are identical.

#### 4.3.2. Reverberation time

The method used to calculate reverberation time is Eyring's formula:

$$T_{60} = \frac{0.161V}{-S \ln(1-\bar{\alpha}) + 4mV}, \quad (10)$$

where  $T_{60}$  is the reverberation time in the space,  $V$  is the volume of the space,  $S$  is the total absorption area of the space,  $\bar{\alpha}$  is the average absorption coefficient, and  $4m$  is the air absorption coefficient. In general, because a large indoor space uses less absorption material, the average sound absorption coefficient is low. In this calculation, it is

**Table 3** The pedestrian route choices with multiple sources, 70 evacuees.

Number of evacuees	Exit A	Exit B	Exit C	Exit D	Exit E	Exit F
Scenario 1	19	8	9	7	9	18
Scenario 2	24	6	7	8	9	16
Scenario 3	23	7	6	12	6	15
Scenario 4	22	5	11	8	12	12
Scenario 5	20	10	6	11	6	17
Scenario 6	20	7	9	9	8	17
Scenario 7	16	10	9	10	10	15

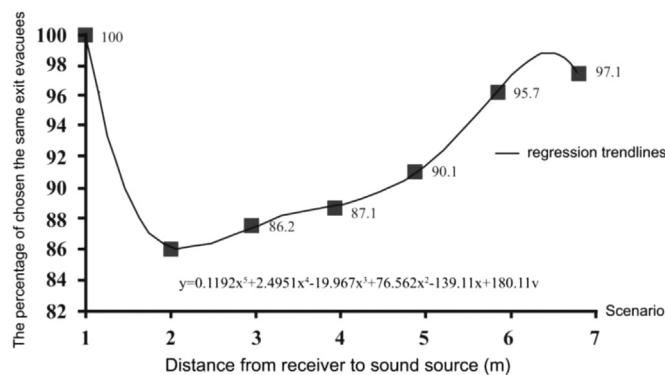


**Figure 6** The percentage of chosen the same exit evacuees in different scenarios.

**Table 4** The pedestrian route choices with multiple sources, 150 evacuees.

Number of evacuees	Exit A	Exit B	Exit C	Exit D	Exit E	Exit F
Scenario 1	30	25	22	21	24	28
Scenario 2	38	22	23	20	22	25
Scenario 3	34	24	24	25	20	23
Scenario 4	35	20	28	22	25	20
Scenario 5	33	26	22	25	20	24
Scenario 6	32	27	27	26	22	26
Scenario 7	29	25	23	22	24	27

assumed that the sound absorption coefficient is 0.2 and the space is squared in plan. Thus,  $T_{60} = 0.12L$ , where  $L$  is the length of the space. The weight of the VWS can then be described as  $l_{j,k} = T \cdot \lg \frac{1}{r}$ .

#### 4.4. Other parameters

There are multiple exits with evacuation alarm sources in a large indoor space. The theory of sound transmission shows that, in general, the nearest voice warning to people will be heard first and may lead people to choose the nearest exit. This statement may not be justified and is not in line with current human behaviour in the fire literature as other exits will disturb the crowd's route choice. This issue needs to be discussed. Experiments with multiple exits with alarm sources have been performed, as described in Section 3.2.2.

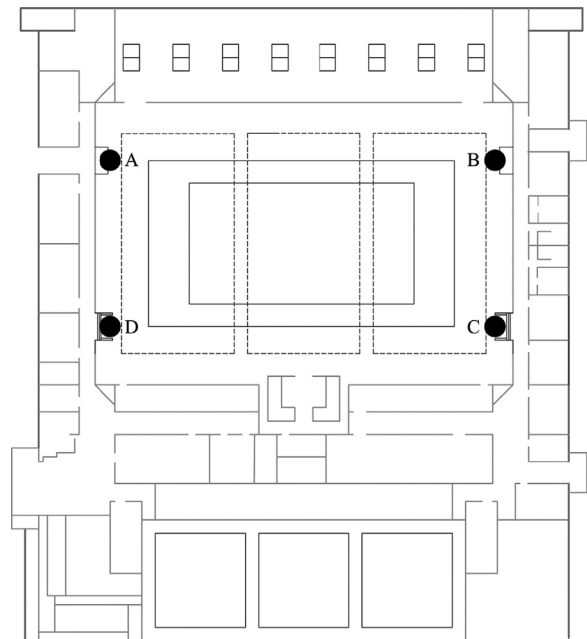
The individual evacuation activities of the six evacuees were recorded and analysed. Figure 3(a) shows the evacuees' position. As indicated above, one quarter of the ground floor was taken as experiment field, shown in Figure 2 (shadowed areas). Differences regarding the evacuation routes and travel distance were studied with different numbers of loudspeakers. Scenario 1 had no loudspeaker in any exit. Scenario 2 had one loudspeaker in Exit A. Scenario 3 had two loudspeakers in Exit A and Exit D. Scenario 4 had three loudspeakers in Exit A, Exit C and Exit E. Scenario 5 had four loudspeakers in Exit A, Exit B, Exit D and Exit F. Scenario 6 had five loudspeakers in Exit A, Exit B, Exit C, Exit D and Exit F. Scenario 7 had loudspeakers in each exit. The evacuation time and route of each evacuee were recorded.

Before the experiment, all exit possibilities were explained to the evacuees. Table 3 shows the results of the multiple source experiment and the number of evacuees through each exit that were recorded.

In Scenario 2, 84.4% of evacuees chose the previous exits. In Scenario 3, 86.2% of evacuees chose the previous exits. In Scenario 4, 87.1% of evacuees chose the previous exits. In Scenario 5, 90.1% of evacuees chose the previous exits. In Scenario 6, 95.7% of evacuees chose the previous exits. In Scenario 9, 97.1% of evacuees chose the previous exits. The number of loudspeakers influenced the choice of exit.

**Table 5** The pedestrian route choices with multiple sources, 300 evacuees.

Number of evacuees	Exit A	Exit B	Exit C	Exit D	Exit E	Exit F
Scenario 1	58	44	48	45	46	59
Scenario 2	66	47	43	44	45	55
Scenario 3	64	42	46	49	46	53
Scenario 4	60	44	51	46	52	47
Scenario 5	58	50	41	52	43	56
Scenario 6	55	52	48	49	44	52
Scenario 7	52	51	49	48	46	54

**Figure 7** The exits (dots) of the gymnasium in observation experiment.

The variable  $f_{i,j}$  can be described as

$$f_{i,k} = g_{j,k}(\eta_{j,k} \cdot l_{j,k}), \quad (11)$$

where  $\eta_{j,k}$  is the VWS factor, the value shown in Figure 6.

Tables 4 and 5 shows the results of the multiple source experiment with 150 evacuees and 300 evacuees. The number of evacuees through each exit was recorded.

In Test A, 61.8% of the evacuees chose the same exit in Scenario 1 and Scenario 6. In Test B, 75.8% of the evacuees chose the same exit in Scenario 1 and Scenario 6. In Test B, 83.1% of the evacuees chose the same exit in Scenario 1 and Scenario 6. The data show that as the number of evacuees increased, the influence of the loudspeakers decreased. Formula (11) considers the influence of the number of evacuees. The variable  $f_{i,j}$  can be described as

$$f_{i,k} = g_{j,k}(\eta_{j,k} \cdot \lg n \cdot l_{j,k}), \quad (12)$$

where  $n$  is the number of evacuees in the current evacuation time.

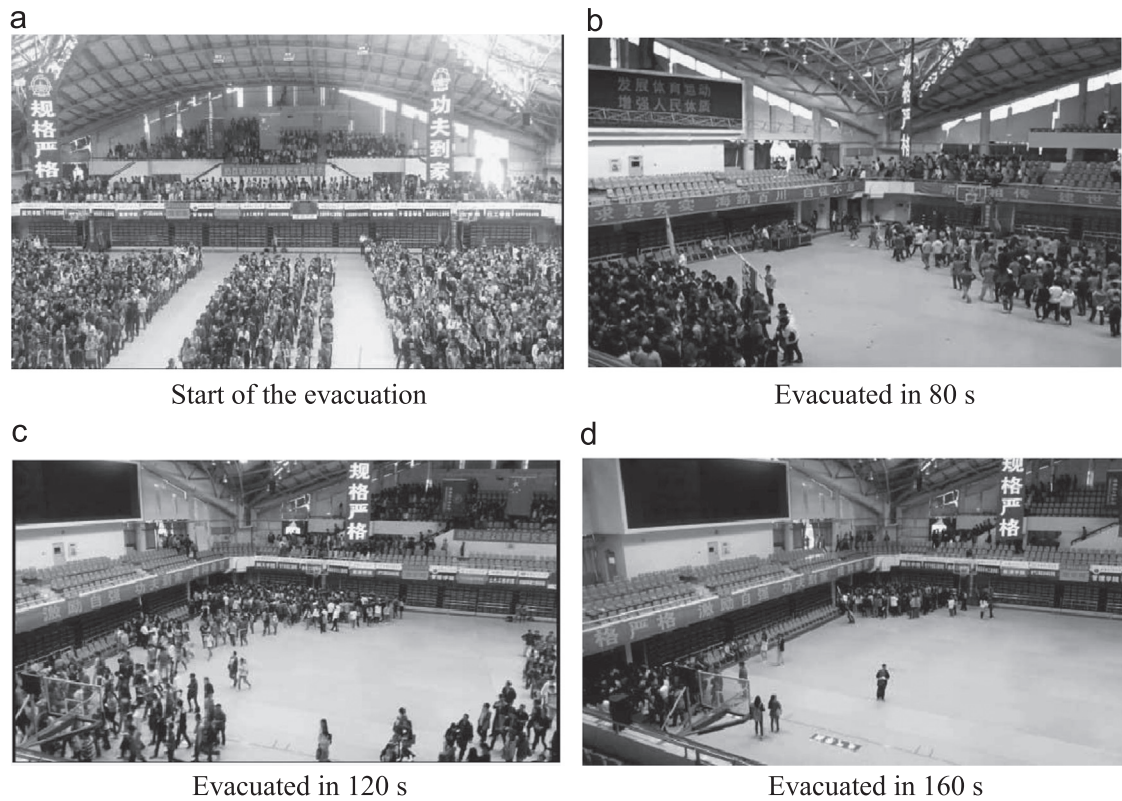


**Figure 8** The evacuation process at different times in the gymnasium.

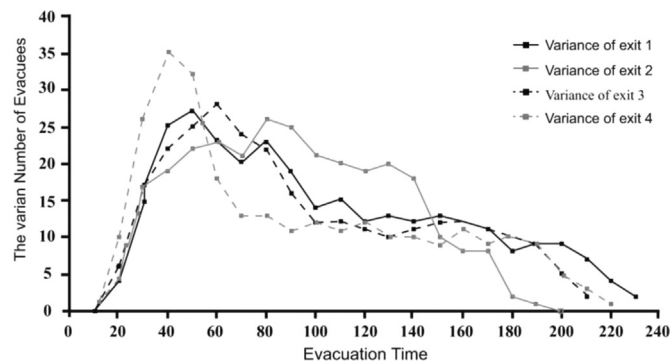


**Figure 9** Variance of the number of evacuees through each exit in the experiment.

## 5. Model validation and application

According to the numerical model and discussion of parameters, a crowd's route choice model was built. This section will validate the CACR model developed above.

### 5.1. Evacuation observation experiment

The CACR model can be used under different circumstances, such as a fire situation or when a different voice warning system is used, which other commercial models cannot simulate. To verify the simulation accuracy of the CACR

model, an observation experiment under high density crowds was chosen for comparison.

The building for the simulation is the gymnasium in the Harbin Institute of Technology, which is used for the test evacuation in Section 3. The gymnasium has four exits open on the ground floor for evacuation, shown in Figure 7, and 1127 spectators were allocated. The response time after receiving the evacuation order is 10 s.

Figure 8 shows the evacuation process at different times in the gymnasium, and Figure 9 shows the variance of the number of evacuees through each exit by observation. The evacuation ability of each exit is not average, but the evacuation process of each exit is nearly the same. The

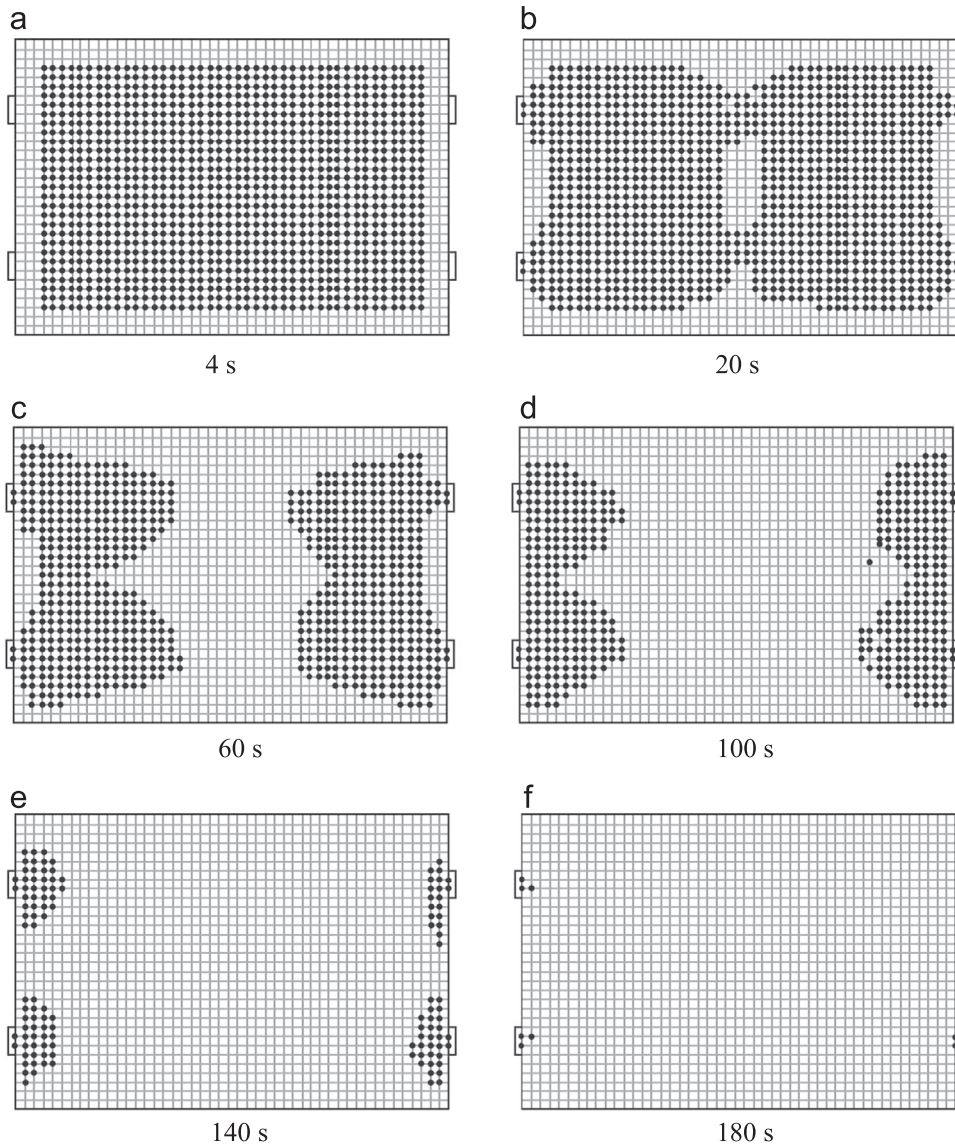


Figure 10 Evacuation simulation using the CACR model.

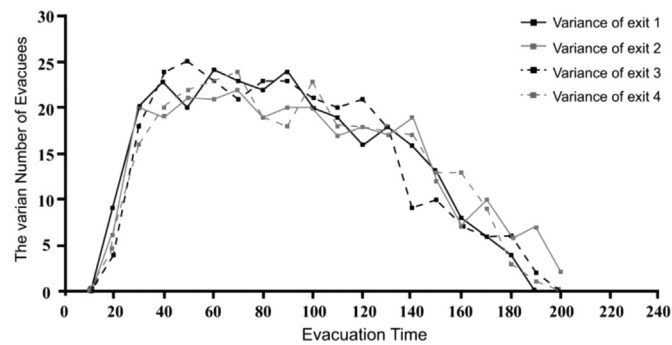
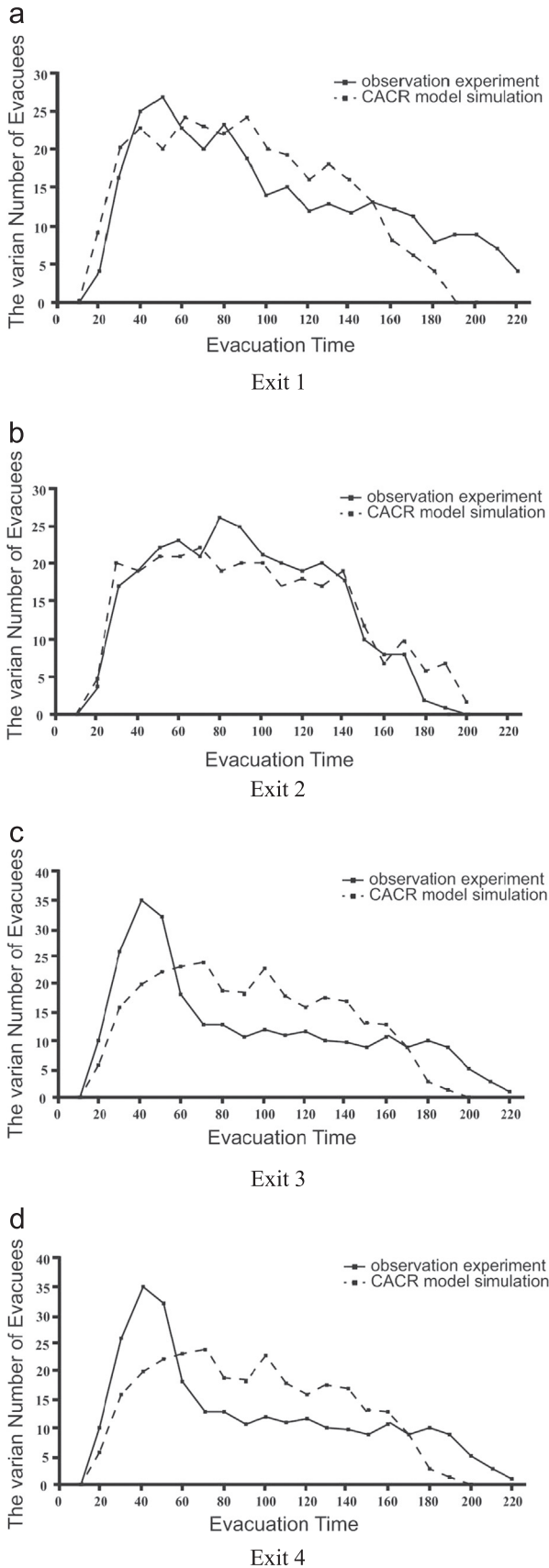


Figure 11 Variance of the number of evacuees through each exit using CACR model.

number of evacuees is low in the first 20 s but increases per unit of time. With crowds gathering at the exits and limited evacuation capacity, the number of evacuees starts to level off at approximately three people per second. After 100 s, the variance of the number of evacuees starts to flatten to

approximately 1.5 people per second. After 180 s, the number of evacuees begins to decline until the evacuation process is completed. The results show that total evacuation time is 3 min 52 s, and the number of evacuees using each exit is very similar. The time of evacuation of exit 2 is



**Figure 12** Comparison of the number of evacuees per unit time by observation experiment and CACR model simulation from each exit.

shorter than the others, and the fluctuating range of variance of exit 4 shows a curve higher than the others.

## 5.2. Evacuation simulation experiment

Figure 10 shows the simulation process at different times by the CACR model. All settings are the same as the observation experiment. The number of evacuees is initially low; after a quick rise, it levels off. Finally, the number decreases slightly, so the process of evacuation is nearly the same as the observation before 20 s and after 160 s. The difference is that the CACR model cannot show good precision when a jam occurs.

Figure 11 shows the variance of the number of evacuees through each exit based on the data of the evacuation simulation. The result shows that the total evacuation time is 3 min 18.8 s. This illustrates that the closer the numbers of evacuees are to the average, the less time the evacuation process takes.

## 5.3. Results comparison

Based on the data from the evacuation observation, the variance of the number of evacuees for each 10 s was calculated for comparison with the CACR models. Values under 1 account for 22%, values above 1 and less than 3 account for 21%, values above 3 and less than 5 account for 27%, values above 5% and less than 10 account for 26%, and values above 10 account for 3%. The maximum value is 15, and the minimum value is 0, which is equal to the average. Values above 5 indicate that the numbers of evacuees at that unit time (10 s) are substantially different from the average.

Figure 12 (a)-(d) shows the number of evacuees from exit 1 to exit 4 for each unit of time. The ratio of the maximum difference to the average value is used to compare the simulation accuracy. The maximum in Figure 12(a) is at 190 s and 200 s, the difference is 9 evacuees, and the ratio of the maximum difference and the average value is 9.4%. In Figure 12(b), the maximum difference is at 80 s, which represents 7 evacuees, and the ratio of the maximum difference and the average value is 15.2%. The maximum in Figure 12(c) is at 120 s, the difference is 10 evacuees, and the ratio of the maximum difference and the average value is 11.1%. In Figure 12(d), the maximum difference is at 40 s, which represents 15 evacuees, and the ratio of the maximum difference and the average value is 11.1%. At 70 s and 100 s, the difference is 11 evacuees, and the ratio is 8.1%. At 30 s and 50 s, the difference is 10 evacuees, and the ratio is 7.4%. Figure 13 shows the average number of evacuees from all exits for each unit of time; the maximum difference is at 100 s, which is 25 evacuees, and the ratio of the maximum difference and the average value is 10.8%. The other values are approximately similar to each other. Instances in which the ratio of the difference and the average value is under 10% account for 80% of the data. The simulation results of each exit using the CACR model are closer to the average.

The main reason for the few relatively large differences in the simulation results by the CACR model is that less

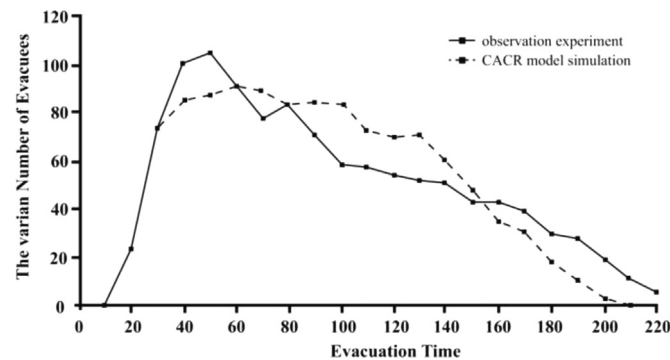


**Figure 13** The comparison of the average number of evacuees through all exits per unit time by observation experiment and CACR model simulation.

consideration was given to the jam. However, the differences are still within an acceptable range.

## 6. Conclusions

In this paper, a route choice model integrating a voice warning system in large indoor spaces was developed. Through the development of the model, a series of phenomena were observed.

The processes of the evacuees' movements were observed, and it seems that different environmental evacuation conditions lead to different evacuation processes. Although most of the evacuees choose the same exit route, walking velocities through different sections are significantly different. Some special environment changes can affect evacuation times and route choices. The experimental results demonstrate that exit route elements, visibility, and voice warning systems have a considerable influence on the average velocities.

A cellular automaton crowd route choice model (CACR model) was developed. The variables of the CACR model were validated through sound field tests and evacuation experiments. The results of the evacuation experiments with a voice warning system show that the number and location of alarms affect route choice.

An observation experiment in a large stadium was employed to test the accuracy of the CACR model in stadium evacuation scenarios. The model was found to be highly accurate, and its results were satisfactory. An application of the CACR model was demonstrated.

## Acknowledgements

The authors are indebted to Professor Shanshan Zhang, Chao Wang, and Shanshan Nie for useful discussions. The work is financially supported by the National Natural Science Foundation of China (NSFC) (51378139).

## References

- Ashe, B., Shields, T.J., 1999. Analysis and modelling of the unannounced evacuation of a large retail store. *Fire Mater.* 23, 333-336.
- Bruck, D., 2001. The who, what, where and why of waking to fire alarms: a review. *Fire Saf. J.* 36, 623-639.
- Bryan, J.L., 2002. *SFPE Handbook of Fire Protection Engineering 3rd edition* National Fire Protection Association, Quincy, MA.
- Burstedde, C., Klauck, K., Schadschneider, A., 2001. Simulation of pedestrian dynamics using a two dimensional cellular automaton. *Physica A* 295, 507-525.
- Fang, Z.X., Li, Q.Q., Li, Q.P., Han, L.D., Wang, D., 2011. A proposed pedestrian waiting-time model for improving space-time use efficiency in stadium evacuation scenarios. *Build. Environ.* 46, 1779-1784.
- Frantzich, H., Nilsson, D., 2003. Utrymning genom tät rök: beteende och förflyttning [Evacuation in dense smoke: behaviour and movement] Technical Report 3126.
- Gwynne, S., Galea, E.R., Owen, M., 1999. A review of the methodologies used in evacuation modelling. *Fire Mater.* 23, 383-388.
- Helbing, D., Farkas, I., Vicsek, T., 2000. Simulating dynamical features of escape panic. *Nature* 407, 487-490.
- Henderson, L.F., 1971. The statistics of crowd fluids. *Nature* 229, 381-383.
- Hoogendoorn, S.P., Bovy, P.H.L., 2003. Pedestrian travel behaviour modelling, In: K. Axhausen (ed.). *Moving through Nets: The Physical and Social Dimensions of Travel* 10th International Conference on Travel Behaviour Research. Lucerne, Switzerland.
- Jeon, G.Y., Hong, W.H., 2009. An experimental study on how phosphorescent guidance equipment influences on evacuation in handicapped visibility. *J. Loss Prev. Process Ind.* 22, 934-942.
- Jin, T., 2008. Visibility and Human Behavior in Fire Smoke. In: *SFPE Handbook of Fire Protection Engineering 3rd edition* National Fire Protection Association, Quincy, MA(USA), pp. 2-42 (2-53).
- Kobes, M., 2010. Way finding during fire evacuation: an analysis of unannounced fire drills in a hotel at night. *Build. Environ.* 45 (3), 537-548.
- Kobes, M., Helsloot, I., deVries, B., Post, J.G., 2010. Building safety and human behaviour in fire: a literature review. *Fire Saf. J.* 45, 537-548.
- Lovas, G.C., 1994. Modelling and simulation of pedestrian traffic flow. *Transp. Res. B* 28 (6), 429-443.
- Mac, H.A., Regan, M.A., Ware, R., 1999. An engineering model for the estimation of occupant pre movement and response time. *Fire Mater.* 23, 255-263.
- Milazzo, J.S., Roupail, N.M., Hummer, J.E., 1998. Effect of Pedestrians on the Capacity of Signalized Intersections. Transportation Research Board. National Research Council, Washington DC.
- Nuria, P., Ali, M., 2008. Evacuation simulation models: challenges in modelling high-rise building. *Autom. Constr.* 2, 377-388.
- Pereira, L.A., Duczmal, L.H., Curz, F.R.B., 2013. Congested emergency evacuation of a population using a finite automata approach. *Saf. Sci.* 51, 267-272.

- Pires, T.T., 2005. An approach for modelling human cognitive behaviour in evacuation models. *Fire Saf. J.* 40, 177-189.
- Pu, S., Zlatanova, S., 2005. Evacuation route calculation of inner buildings. In: Oosterom, P.V., Zlatanova, S., Fendel EM, E.M. (Eds.), *Geo-information for Disaster Management*. Springer Verlag, Berlin, Germany, pp. 1143-1161.
- Ramachandran, G., 1991. Informative fire warning systems. *Fire Technol.* 27, 66-81.
- Ronchi, E., Gwynne, S.M.V., Purser, D.A., Colonna, P., 2013. Representation of the impact of smoke on agent walking speeds in evacuation models. *Fire Technol.* 49, 411-431.
- Sekizawa, A., Ebihara, M., Notakeet, H., 1999. Occupants' behaviour in response to the high-rise apartments fire in Hiroshima City. *Fire Mater.* 23, 297-303.
- Shi, J.Y., Ren, A.Z., Chen, C., 2009a. Agent-based evacuation model of large public buildings under fire conditions. *Autom. Constr.* 18, 228-241.
- Shi, J.Y., Ren, A.Z., Chen, C., 2009b. Agent-based evacuation model of large public buildings under fire conditions. *Autom. Constr.*, 338-347.
- Sime, J.D., 2001. An occupant response shelter escape time (ORSET) model. *Saf. Sci.* 38, 109-125.
- Tong, A.D., Canter, D., 1985. The decision to evacuate: a study of the motivations which contribute to evacuation in the event of fire. *Fire Saf. J.* 9, 257-265.
- Wolfgram, S., 1983. Statistical mechanics of cellular automata. *Rev. Mod. Phys.* 55, 601-644.
- Yang, L.Z., Zhao, D.L., Li, J., Fang, T.Y., 2005. Simulation of the kin behaviour in building occupant evacuation based on Cellular Automaton. *Build. Environ.* 40, 412-422.
- Zhao, D.L., Li, J., Zhu, Y., Zou, L., 2008. The application of a two-dimensional cellular automata random model to the performance-based design of building exit. *Build. Environ.* 43, 518-522.
- Zheng, X.P., Sun, J.H., Cheng, Y., 2010. Analysis of crowd jam in public buildings based on cusp-catastrophe theory. *Build. Environ.* 45, 1755-1761.